

Correspondent: J. Steinberger  
CERN  
1211 Geneva 23  
Switzerland

PROPOSAL FOR A MEASUREMENT OF THE MOMENTUM DEPENDENCE  
OF THE DIFFERENCE IN FORWARD SCATTERING AMPLITUDES  
OF  $K$  AND  $\bar{K}$

W. Carithers, D. Nygren, Columbia University, New York

J. Steinberger, Columbia University, New York and  
CERN, Geneva, Switzerland

D. Dorfan, C. Heusch, C. Prescott, University of California  
at Santa Cruz

N. Gelfand, University of Chicago, Chicago, Ill.

K. Kleinknecht, University of Heidelberg, Heidelberg, Germany

H. Wahl, CERN, Geneva, Switzerland

June, 1970

Proposal for a Measurement of the Momentum Dependence  
of the Difference in Forward Scattering Amplitudes  
of  $K$  and  $\bar{K}$

W. CARITHERS, D. NYGREN, Columbia University, New York.

J. STEINBERGER, Columbia University, New York, and  
CERN, Geneva, Switzerland.

N. GELFAND, University of Chicago, Chicago, Ill.

K. KLEINKNECHT, University of Heidelberg, Heidelberg, Germany.

H. WAHL, CERN, Geneva, Switzerland.

## I. INTRODUCTION

The difference,  $f-\bar{f}$ , in the forward scattering amplitude of particles and their antiparticles has been the subject of substantial interest. Pomeranchuk<sup>1</sup> predicted, on the basis of assumptions concerning the analyticity of the scattering amplitudes that  $f-\bar{f}$  should asymptotically approach zero at high energy. The indications at energies below  $\sim 20$  BeV favor the validity of the theorem. It will therefore be interesting to see how the differences ( $f-\bar{f}$ ) behave at higher energies.

The Pomeranchuk theorem predicts the high energy asymptotic value of  $f-\bar{f}$ , but it does not predict the rate of approach to this value. However, dynamical models<sup>2</sup> using Regge poles have been put forward which predict that the rate of approach should be as  $p^{-1/2}$  and that the ratio  $\frac{\text{Re}(f-\bar{f})}{\text{IM}(f-\bar{f})}$  should approach unity at high energies. The latter prediction can also be stated as follows:  $\phi_{f-\bar{f}} = \text{Arg}(f-\bar{f}) = 45^\circ$  or  $135^\circ$ . Both of these predictions are in reasonable agreement with present data. See for instance Fig. 1 for a compilation of cross section data.

In the measurement of ( $f-\bar{f}$ ) the commonly used technique is to measure the total cross sections for particle and antiparticle, and relate these to  $\text{Im } f$  and  $\text{Im } \bar{f}$  with the help of the optical theorem. In this way a not unreasonable accuracy, perhaps  $\sim 10\%$ , can be achieved also at NAL energies. On the other hand, the determination of  $\text{Re}(f-\bar{f})$  requires delicate coulomb interference experiments with positive and negatively charged particles and meaningful results may not be achievable at NAL energies.

In the case of the  $K^0$  and  $\bar{K}^0$  mesons, however, the

regeneration phenomenon permits the measurement of  $(f-\bar{f})$ , both magnitude and phase, with remarkable accuracy.<sup>3</sup>

A beam of  $K_L$ , on traversing matter, will produce  $K_S$  with a relative amplitude  $\rho$  where

$$\rho = \frac{\pi i (f-\bar{f})}{k} ND \left( \frac{1 - e^{i\Delta\Gamma D m/k}}{-i\Delta\Gamma D m/k} \right) \quad (1)$$

and

$k$  = kaon momentum

$N$  = nuclear density

$D$  = thickness of converter

$$\Delta M = (m_L - m_S) - i(\Gamma_L - \Gamma_S)/2$$

$$m = (m_L + m_S)/2$$

The regeneration is proportional to the difference in the forward scattering amplitudes. Furthermore, if this regeneration is detected by means of the  $\pi^+\pi^-$  decay, the interference between the short and long-lived two pion decays is also observed. The time dependent two pion intensity is given by the expression

$$I_{2\pi}(\tau) = |\rho|^2 e^{-\Gamma_S \tau} + 2|\rho\eta| e^{-\bar{\Gamma}\tau} \cos(\Delta m\tau + \phi_\eta) + |\eta|^2 e^{-\Gamma_L \tau} \quad (2)$$

where  $\eta = \langle \pi^+\pi^- | T | L \rangle / \langle \pi^+\pi^- | T | S \rangle$

$\tau$  = proper time of kaon after traversal of regenerator

$$\bar{\Gamma} = (\Gamma_L + \Gamma_S)/2$$

$$\Delta m = (m_L - m_S)/2$$

$$\phi_\rho = \text{Arg}(\rho)$$

and  $\phi_\eta = \text{Arg}(\eta)$ .

In Fig. 2 we have plotted expression (2) for the case of 100 BeV/c kaons, a cross section difference of 0.5 mb, a liquid H<sub>2</sub> target length of 5 m, and for various values of  $\text{Re } \Delta f / \text{Im} \Delta f$ . Experimental uncertainties which might reasonably be expected are also indicated for one of the curves.

It may be worthwhile to note two interesting aspects:

1. The expected decrease in  $(f - \bar{f})$  with momentum, that is,  $(f - \bar{f}) \propto p^{-1/2}$ , is more than offset by the kinematic effect of the longer laboratory lifetime, so that the regeneration amplitude  $\rho$ , Eq. 1, for a target of optimum length is actually expected to increase with energy. The experiments are therefore expected to be easier at NAL energies than at lower energies. 2. The expected amplitude differences are still quite substantial, even at the highest NAL energies, and decreasing slowly with energy. It seems therefore unrealistic to consider the proposed experiment as a critical test of the Pomeranchuk theorem. Instead it should be considered as a measurement of the dynamics, the precise way in which asymptopia is approached.

## II. APPARATUS

The proposed apparatus is based on one presently under construction for a measurement of the  $\eta_{+-}$  phase at Brookhaven National Laboratory. It must, however, be modified to optimize it for higher momenta. These modifications consist chiefly of:

- a) appropriate lengthening of the decay region and spectrometer
- b) conversion of the Cerenkov counter to He from H<sub>2</sub>
- c) addition of a shower detector
- d) addition of a fourth wire chamber plane.

With these modifications it will make an excellent detector at NAL. A layout is shown in Fig. 3.

The vertical and horizontal scales of this figure are not the same. The longitudinal dimensions have been matched to the kaon momentum band 40-100 BeV/c, and may require modifications depending on the beam that will be actually available. We briefly discuss the component parts other than the beam itself:

1. Target

The target is a liquid hydrogen (alternately deuterium) container. The optimum length is proportional to the momentum, in order to maximize  $|\rho|$  (Eq. 1). At 100 BeV/c, a target length of 5-6 m is indicated. The same target will also serve well at lower momenta, so that it will be possible to get the data for a wide momentum band in a single run.

2. Decay Path

Since it is informative to study the interference (Eq. 2, Fig. 2) for a proper time interval of at least  $\sim 8 \tau_s$ , the decay length should be at least  $\sim 40 \text{ cm} * P_K(\text{BeV})$ , or  $\sim 40 \text{ m}$  at 100 BeV/c. It should have a minimum of matter. A vacuum would require a relatively thick window on the

proportional chamber which follows, so that atmospheric helium or hydrogen throughout the apparatus, is preferable. In our apparatus, the helium tanks are flanged directly to the wire chambers, so that there is a single 1 mil mylar window separating the two. The total amount of matter traversed on the average by the decay secondaries in the decay region and spectrometer is  $0.96 \text{ g/cm}^2$ , almost entirely helium.

### 3. Spectrometer

The spectrometer consists of a magnet preceded and followed by two proportional wire planes. The total is enclosed in a helium container which threads also the magnet. The section between wire plane 3 and 4 acts as an atmospheric He Cerenkov counter.

a. Magnet. The magnet is a joint BNL-Columbia effort and has an aperture of 96 in. x 22 in. It requires 4000 amps at 140 volts, and is expected to be capable of imparting a transverse momentum change of 350 MeV/c.

b. Charpak Chamber. All planes employ a wire spacing of 2 mm, corresponding to a spatial resolution  $\sigma = \pm 0.7 \text{ mm}$ . Plane 2 has only vertical wires, the others have both vertical and horizontal wires. Together there are approximately 6500 wires. Each wire is followed by an amplifier and pulse former mounted in proximity. The signals are then transmitted to a central electronics station where they are gated and stored for reading into the computer. The transmission cable also serves as delay, so that a preliminary decision can be made before storage. Only events meeting certain simple requirements are stored. The

fundamental time resolution of the chambers and amplifiers is  $\sim 20$  nsec, and we expect to achieve an overall resolution for the entire proportional wire system of  $\sim 40$  nsec. The time required to reject a stored event, or read it into a buffer for subsequent transmission to the computer is  $\sim 200$  nsec.

c. Geometric efficiency and resolution. Monte Carlo calculations on two pion detection have been performed for the geometry of Fig. 3, to determine the efficiency as function of proper time and the resolution. The calculations include the effect of multiple scattering in both chamber and gas. The time-dependent efficiencies are shown in Fig. 4. In Fig. 5, as illustration of the resolution, expected mass distributions for  $K \rightarrow \pi^+ \pi^-$  events are shown for several momenta. These calculations represent the effects of measurement error and multiple scattering.

#### 4. C Counter

The region between chambers 3 and 4 acts as an atmospheric He Cerenkov counter. A cross section of the optics is shown in Fig. 6. The flat mirror through which the particles must pass is very thin,  $\sim 1$  mil aluminized mylar. The counter will count electrons of all momenta, and pions above 17 GeV/c. It is used to distinguish electrons from pions, for momenta below this value.

#### 5. Trigger Counters

A plane containing  $2 \times 6 = 12$  scintillation counters, 1/8 in. thick, and covering the area of the last Charpak

chamber, is used to supply a trigger pulse which determines the storage of an event in the Charpak chamber memory unit. These events are then transferred to the magnetic tape units if certain additional properties (such as at least two tracks in each Charpak plane) are met.

We point out here that the step of accepting an event into the chamber memory unit and its possible rejection because of inadequate information content requires only  $\sim 200$  nsec in our case, as against  $\sim 5$  milliseconds in the conventional spark chamber setup. This has two advantages. For one, the trigger which initiates storages can be considerably looser, since little beam time is lost even if a large fraction (say 99%) of these events are rejected before storage on magnetic tape. Secondly, the preselection of events before magnetic storage makes it possible to have a higher percentage of events which will reconstruct.

#### 6. Shower Detector

The Cerenkov counter will not differentiate between electrons and pions above 17 BeV. We therefore insert an electron detector of a simple type behind the trigger counter. It consists of a lead converter sheet, approximately 4 radiation lengths thick, followed by two planes of crossed scintillator strips, 23 cm wide and 5 mm thick. The horizontal strips are broken in the center. Altogether there are 20 counters. High energy showers will produce pulses of the order a hundred times minimum, and

can therefore be selected from pions and muons by the requirement of a large pulse in each plane. The horizontal and vertical counter numbers provide a rough position measurement of the electrons.

#### 7. Muon Detector

This consists of a filter of ordinary concrete  $\sim 5$  m thick, followed by a scintillation counter arrangement of the same general geometry as that of the shower detector. The counter planes are separated by  $\sim 1$  m of concrete. Minimum muon momentum for detection is  $\sim 3$  GeV/c. Discrimination against hadrons and electrons is  $\sim 100\%$ .

#### 8. Computer

The apparatus has a PDP 8 attached, which is used to check the operation of the Charpak chambers and circuits, and the Cerenkov counter. We do not expect to write the magnetic tape with this unit, nor to monitor the data acquisition. For this purpose we require a computing facility, hopefully furnished by NAL, which has a memory capacity of  $\sim 30,000$  18 bit words, or its equivalent.

### III. BEAM, RATES AND RUNNING PERIOD

#### A. Beam Intensity

The beam intensity is limited not by the available intensity, but by the background produced in the

regenerator. The thickness of the regenerator is  $\sim 35 \text{ g/cm}^2$  which is  $\sim 016$  mean nuclear free paths. Secondaries produced in the regenerator give spurious, time uncorrelated tracks in the chambers. A condition on the tolerable level of these spurious tracks then imposes a condition on the maximum tolerable beam flux. The permissible beam flux is therefore inversely proportional to the resolution time (memory time) of the wire chambers. Since this is of the order of 30 times shorter for Charpak chambers than spark chambers in such a long apparatus, the permissible beam intensity, and therefore the data taking rates also, will be  $\sim 30$  times faster for proportional chambers than for spark chambers.

In order to estimate the permissible kaon flux, we assume that there are  $\sim 100$  neutrons/ $K_L$  in the momentum window, that 50% of the neutrons interact, that the interactions produce on the average one track in the wire chambers, and that one can tolerate an average of one spurious track/event. With a 40 nsec resolving time, the permissible  $K_L$  flux is then  $\sim 0.5 * 10^6/\text{sec}$ .

#### B. Beam Location at NAL and Beam Angle.

The design of secondary beams at NAL is not yet completed, so that the alternatives are not as yet clear. There seem to be two possibilities, one a beam at  $\sim 6$  mrad

produced on an internal target, the other at a much smaller angle, at present thought to be  $\sim 1.5$  mrad, produced on an external target. The internal beam has the advantage of being available sooner, but has the disadvantage that the kaon energies which would be available would be lower because of the larger production angle, even if the accelerator is run at higher energy. The latter state of affairs is shown in Fig. 7, where expected  $K_L$  spectra are shown at 6 mrad for both 200 and 400 BeV/c incident proton energy, as well as at 1.5 mrad and for 200 BeV incident protons. All spectra are taken from the calculations of Awshalom and White as quoted by Cocconi<sup>4</sup>.

The spectra fall off rapidly at the high momentum end. In order to get some idea of the upper energy limit available for these three beam conditions, we arbitrarily assume that the beam is useful up to a momentum at which the kaon intensity has fallen to 1/10 of its maximum. These momenta are given in Table I.

Also tabulated are estimated neutron background fluxes, which are considerably higher at small angles, as well as the expected duty cycle, which depends on the circulating beam energy at least for some years yet. The background figure of merit is duty cycle divided by neutron flux. The background favors the larger production angle, but this in our mind is more than offset by the higher available energy at smaller angles. We note here that in the case

of an external target, the available beam intensity is at least an order of magnitude greater than necessary and it would probably be advantageous to introduce a low  $z$  moderator into the beam. The neutron cross sections at these energies are approximately the double of the kaon cross sections, and a moderator which reduces the kaon flux by a factor of  $\sim 10$  would reduce the neutron/kaon ratio by a factor of the order of 5.

On the basis of these considerations, we prefer the external beam solution at the smaller angle.

At 1.5 mrad, and with an aperture of 2 in. x 2 in. at 1500 ft, approximately  $10^{12}$  protons on target are sufficient to produce the maximum tolerable intensity.

### C. Rates

We assume for the moment a proton energy of 200 BeV/c and a neutral beam at  $\sim 1.5$  mrad. The kaon momentum spectrum is expected to peak at approximately 40 BeV/c and fall to perhaps 1/10 of its peak intensity at 130 BeV/c. Perhaps 50% of the kaons will be in the band 40-130 BeV/c.

The "luminosity" of the apparatus can be expressed in terms of the number of  $K_L \rightarrow \pi^+ \pi^-$  decays per short lived lifetime. With the foregoing numbers, the inclusion of an overall loss factor of 50% for failure of reconstruction and other losses, a duty cycle of 20%, and an 18 hour day, the expected rate will be 1000 decays  $K_L \rightarrow \pi^+ \pi^-$  per day per  $\tau_s$  in the momentum interval 40-130 BeV/c. If the momentum band is divided into 10 bins of equal intensity,

then the total signal from a two week run will be of the order of  $1400 K_L \rightarrow \pi^+ \pi^-$  decays per  $\tau_S$  per momentum bin. The time of two weeks should be doubled to include a measurement with deuterium and probably doubled again to make allowance for preliminary measurements, checks, and mistakes. This would bring the total beam time to  $\sim 8$  weeks.

#### D. The Analysis and Accuracy

The problem here is not substantially different from that which has been mastered in the  $K^0 \rightarrow \pi^+ \pi^-$  interference experiments which lead to the determination of the phase of  $\eta_{+-}$ . Systematic problems, such as knowledge of the time-dependent efficiency, and backgrounds due to other decay modes are not expected to be important. The accuracy which can be expected depends on the actual values of the magnitude and phase of  $(f-\bar{f})$ , but is expected to be of the order of one percent in  $|f-\bar{f}|$  and  $\sim 5^\circ$  in the phase for each of the ten momentum bins. Of course, the phase which is measured is  $\phi_{\Delta f} + \phi_\eta$  and it is necessary to know  $\phi_\eta$  to extract  $\phi_{\Delta f}$ . At this time,  $\phi_\eta$  is known to  $4-5^\circ$  accuracy, but at the time of the proposed experiment, it should be known with  $\sim 1^\circ$  accuracy, so that no appreciable error is expected from this source.

#### IV. TIME SCHEDULE

The bulk of the apparatus should be ready at BNL towards the end of 1970. During 1971 and the beginning of 1972, it is expected that measurements leading to a

precise  $\eta_{+-}$  phase will be performed. The most convenient time for transfer to NAL would seem to be towards the middle of 1972. As nearly as we can tell this will fit well into the NAL schedule, but modifications in the BNL schedule are possible and can be discussed.

Concluding Remarks.

1. The measurement of the regeneration amplitude in hydrogen and deuterium, at high momenta, as a function of momentum, would provide useful data on the dynamics of the approach of the forward scattering amplitudes to the Pomeranchuk limit. In this respect the neutral kaon provides a unique experimental opportunity.

2. We believe that the Charpak chamber spectrometer is at present the best apparatus for getting precise data.

3. We propose to bring such an apparatus to NAL, after it has been tested and used at BNL.

4. In order to achieve the highest kaon momenta it will be necessary to work at a correspondingly small beam production angle. In order to achieve this, we would prefer to work in the external beam.

TABLE I

Available kaon momenta and neutron contamination for three possible beam situations.

Beam	Maximum Available Momentum GeV/c	Ratio Neutron flux to kaon flux above 40 GeV/c	Duty Cycle	Background Figure of Merit
200 GeV/c incident proton at 1.5 mrad.	130	70	0.2	0.0029
200 GeV/c incident proton at 6 mrad.	85	24	0.2	0.0083
400 GeV/c incident proton at 6 mrad.	102	5	0.06	0.012

## REFERENCES

- 1 I. Ia Pomeranchuk, Soviet Physics JETP 7, 499 (1958).
- 2 V. Barger, M. Olsson, and D.D. Reeder, Nucl. Phys. B5, 411 (1968).  
F.T. Gilman, Phys. Rev. 171, 1453 (1968).  
B. Margolis, submitted to Kiev Conference.
- 3 K. Kleinknecht, Phys. Letters, 30B, 514 (1969).
- 4 M. Awschalom and T. White, N.A.L. FN191, June 9, 1969.  
These calculations follow the formulas of R. Hagedorn and T. Ranft, Suppl. Nuovo Cimento, 6, 169 (1968).  
The numbers used here are those quoted by G. Cocconi, 1969 Summer Study NAL, Vol. 1, page 397.
- 5 J.V. Allaby, et al, Physics Letters 30B, 500 (1969).

## FIGURE CAPTIONS

- Fig. 1 Momentum dependence of particle and antiparticle cross sections and predictions of Regge Pole models. From Allaby, et al, Ref. 5.
- Fig. 2 Time dependence of  $K_L \rightarrow \pi^+ \pi^- - K_S \rightarrow \pi^+ \pi^-$  interference following a 5 m long  $H_2$  regenerator at 100 GeV/c assuming  $\sigma_{\bar{K}} - \sigma_K = 0.5$  mb and various phases of  $f-\bar{f}$ .
- Fig. 3 Top and side view of proposed layout. Note the difference in transverse and longitudinal scale.
- Fig. 4 Calculated detection efficiencies of the apparatus of Fig. 3 for  $K \rightarrow \pi^+ \pi^-$  decay as function of the kaon proper time, for three values of the kaon momentum.
- Fig. 5 Calculated resolution function in the kaon mass for the decay  $K \rightarrow \pi^+ \pi^-$ . The curves represent the effects of wire chamber resolution and multiple scattering.
- Fig. 6 Section through Cerenkov counter.
- Fig. 7 Expected  $K_L$  fluxes for three different beam conditions according to Awschalom and White.<sup>4</sup>

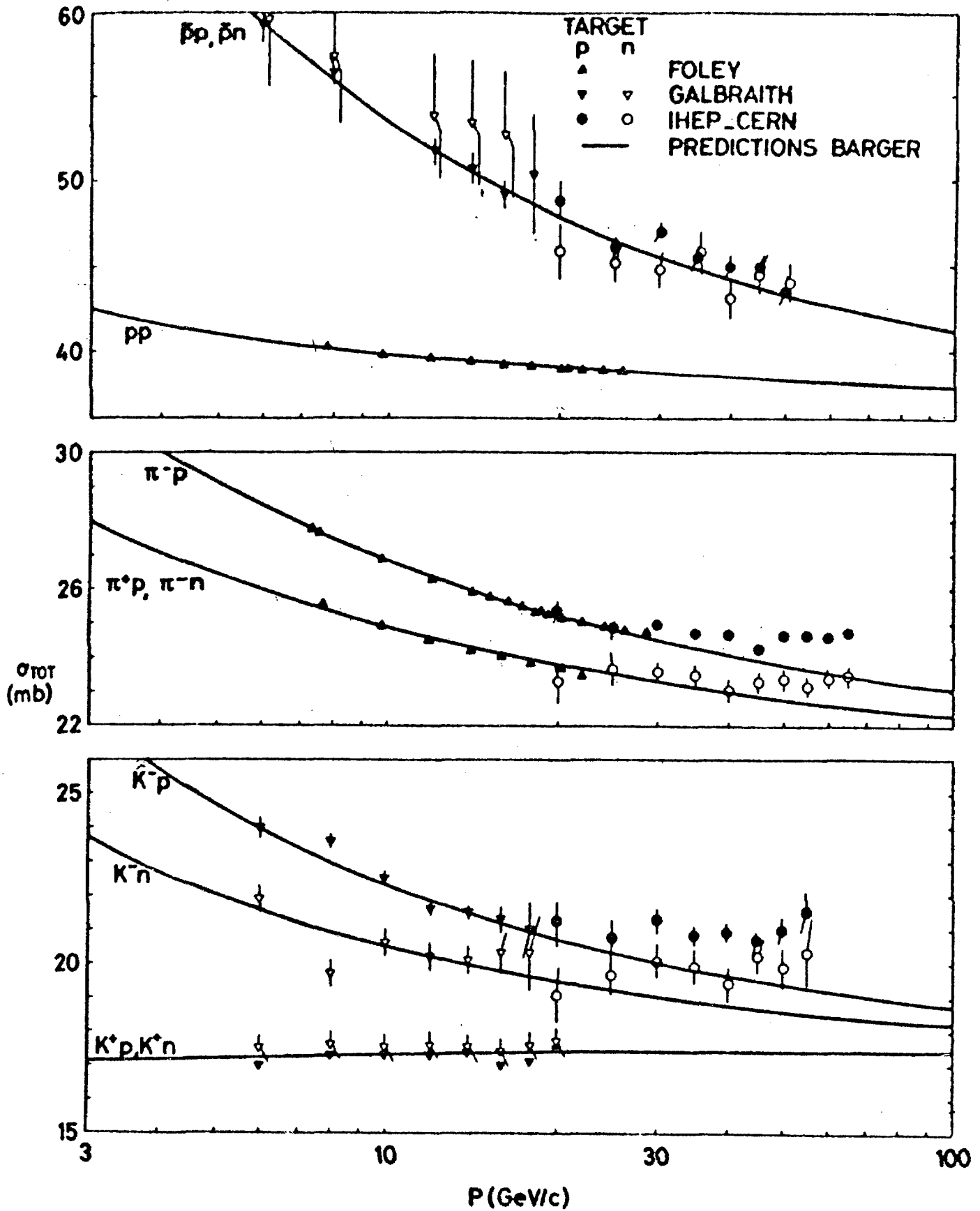


Fig. 1

# TWO PION INTENSITY VS PROPER TIME

$\Delta\sigma = .5 \text{ mb}$

$P_K = 100 \text{ Bev}$

$H_2 \text{ TARGET LENGTH} = 5 \text{ m}$

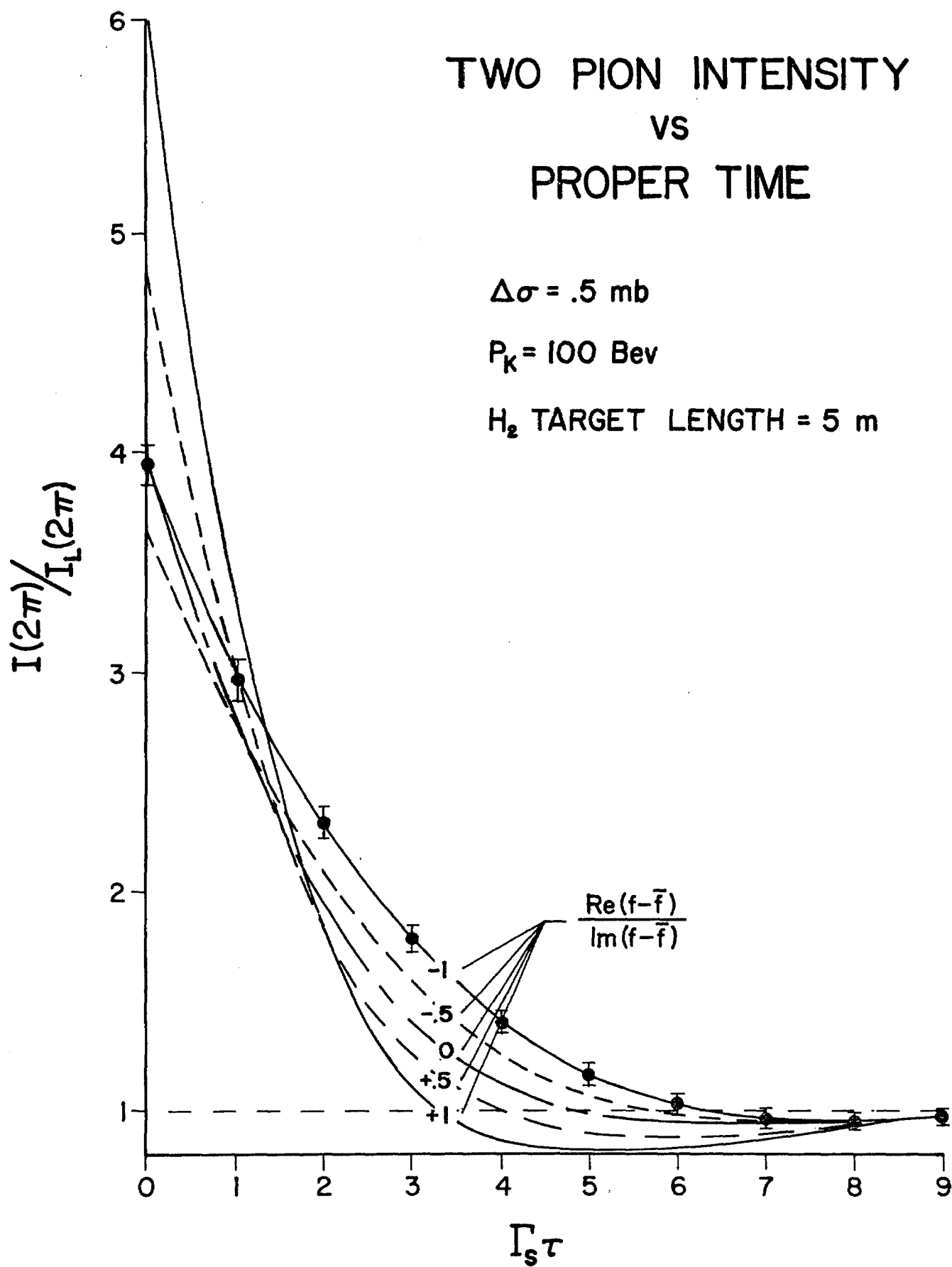


Fig. 2

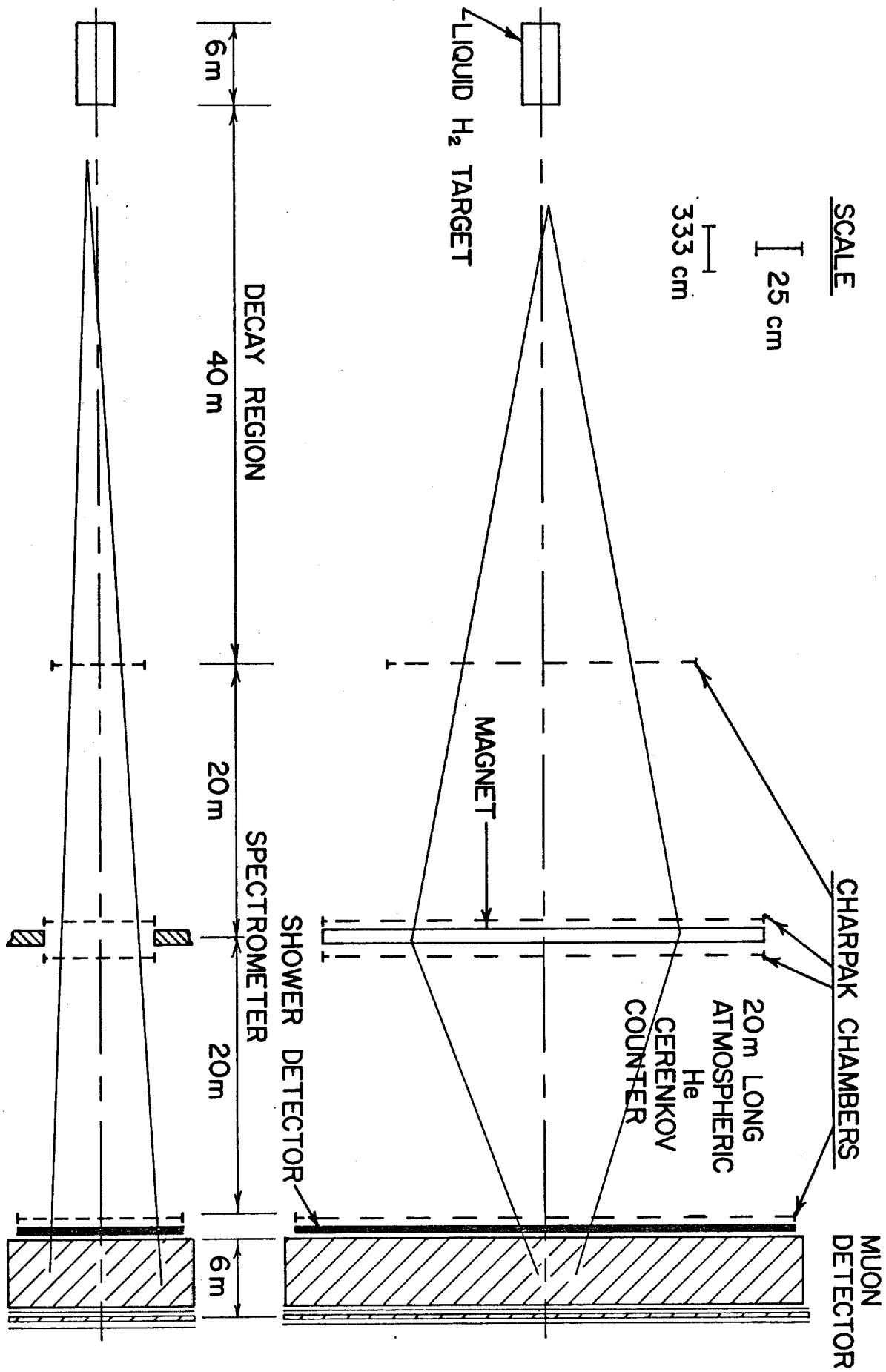


Fig. 3

# DETECTION EFFICIENCY

VS

# PROPER TIME

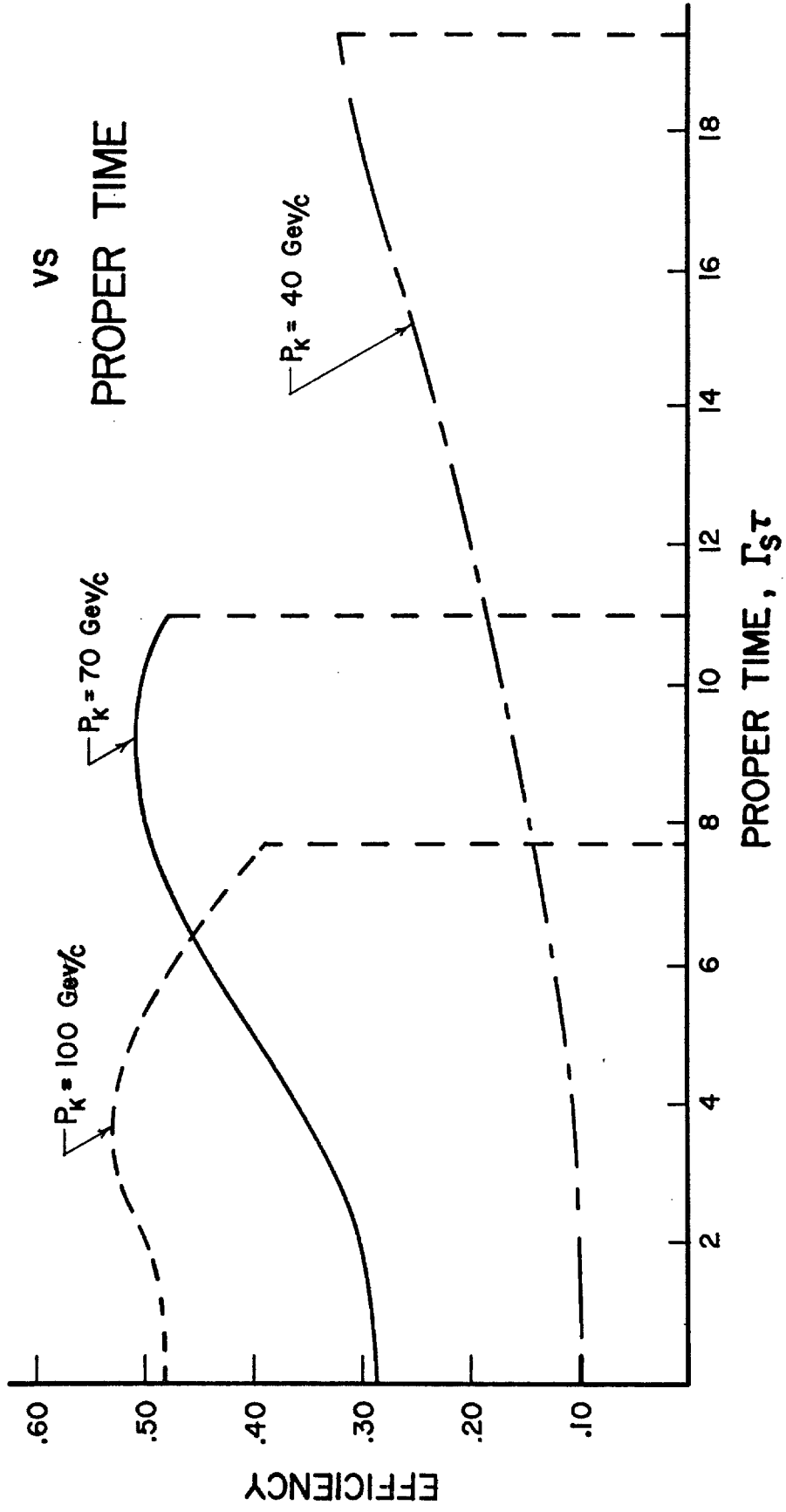


Fig. 4

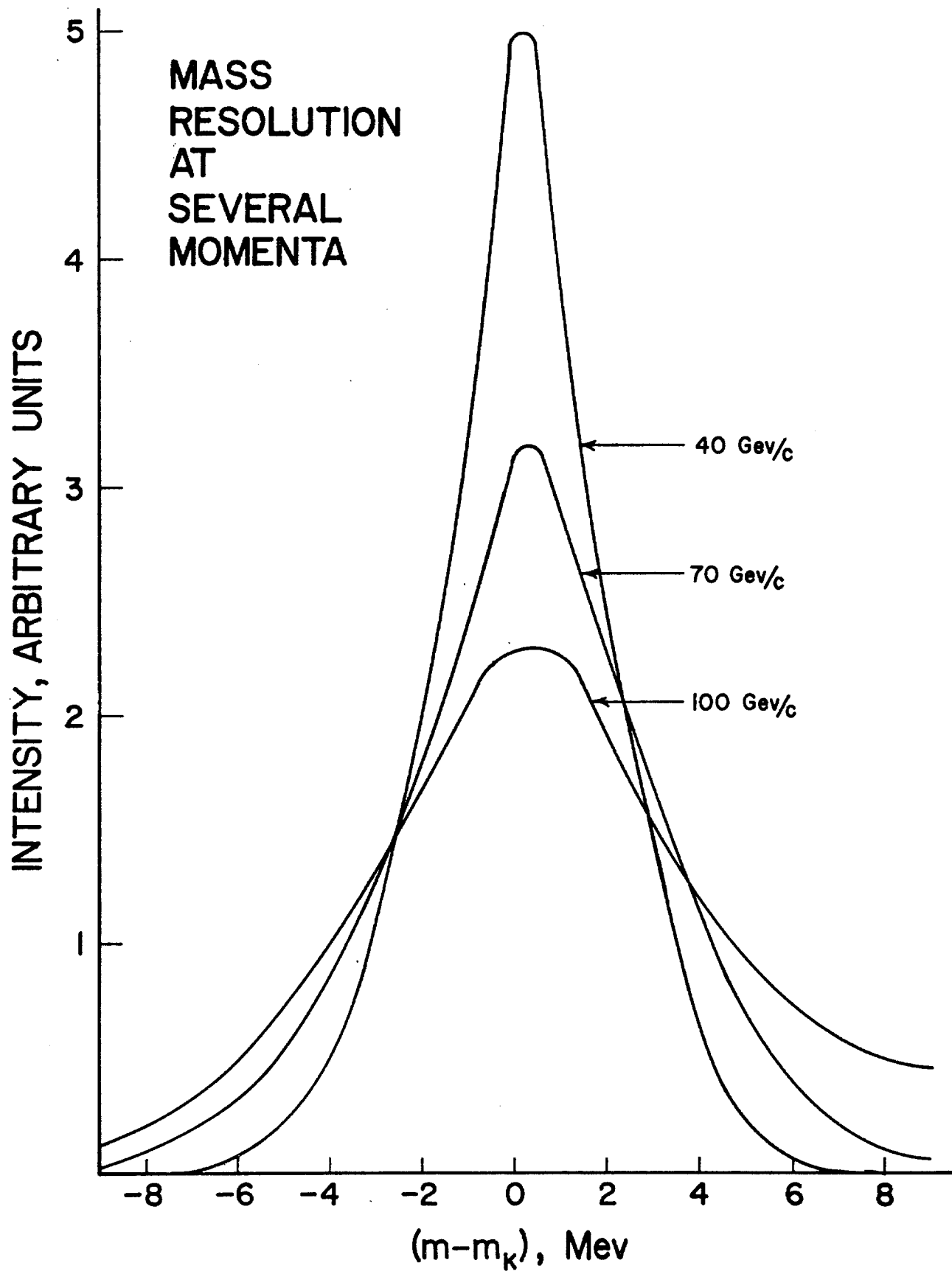
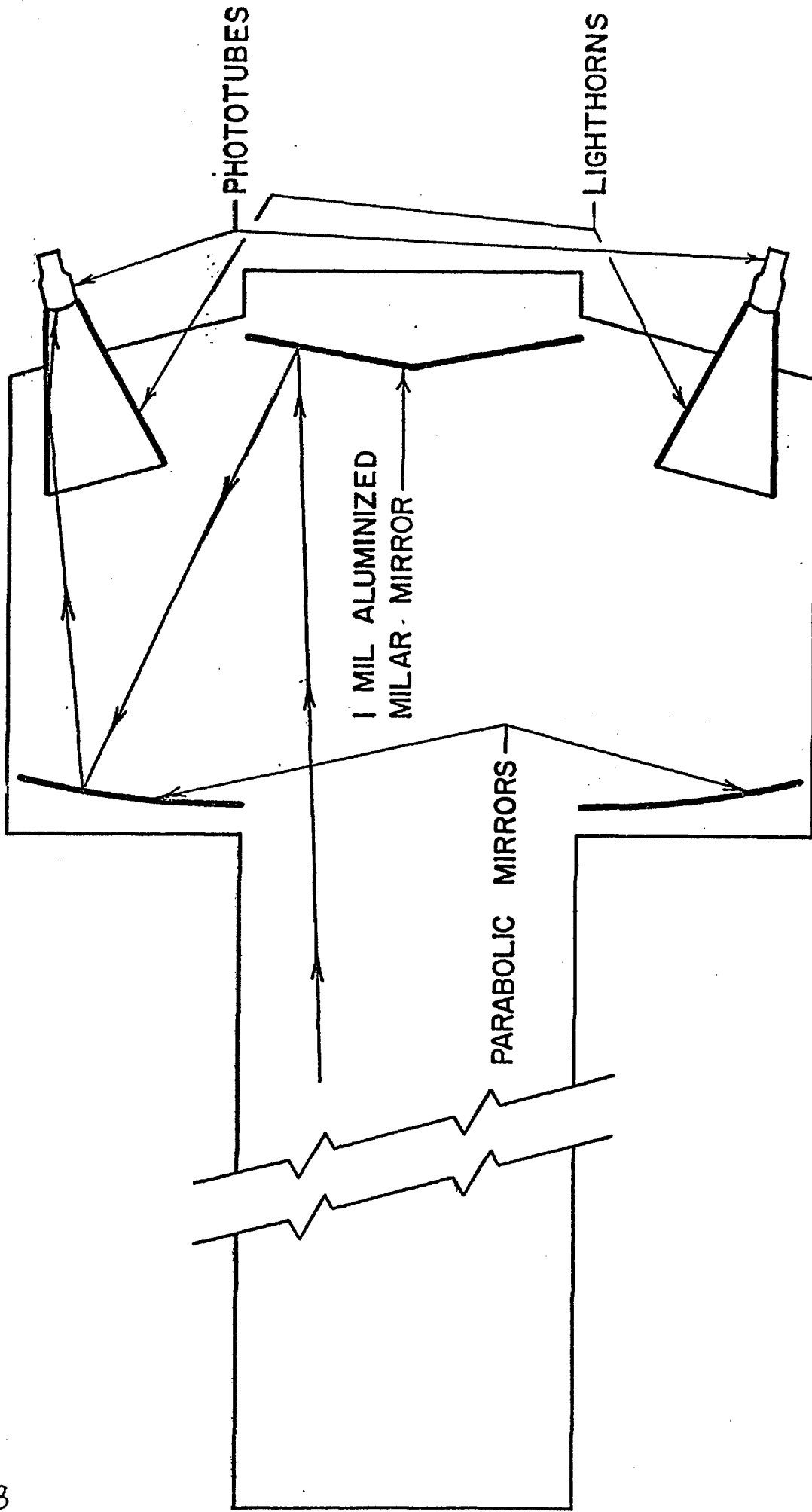


Fig. 5



# SIDE VIEW OF CERENKOV COUNTER

Fig. 6

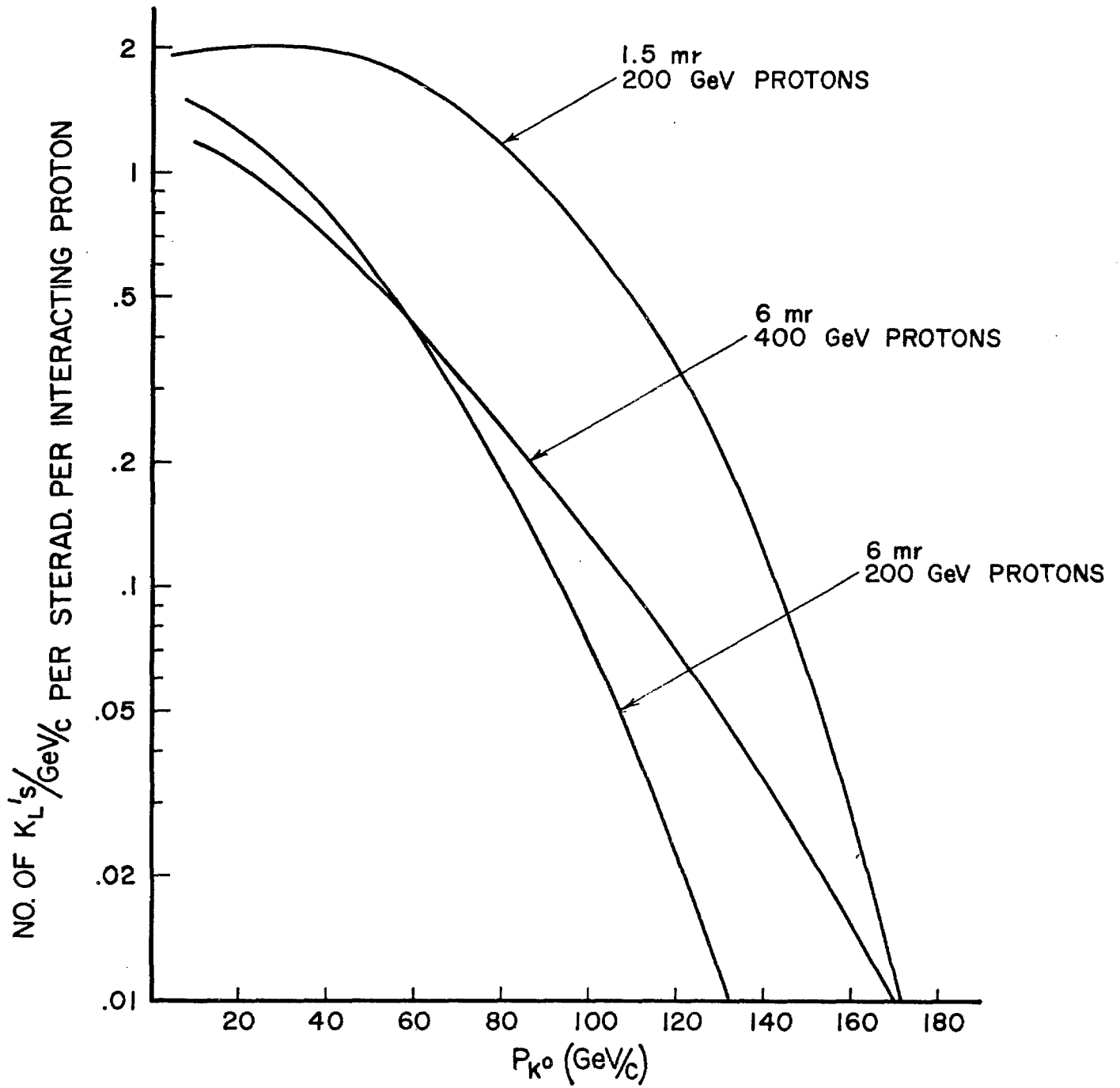


Fig. 7

ADDENDUM TO THE

Proposal for A Measurement of the Momentum Dependence  
of the Difference in Forward Scattering Amplitudes  
of  $K$  and  $\bar{K}$

$K^0$  Charge Radius

W. CARITHERS, D. NYGREN, Columbia University, New York

J. STEINBERGER, Columbia University, New York

CERN, Geneva, Switzerland

N. GELFAND, University of Chicago, Chicago, Ill.

K. KLEINKNECHT, University of Heidelberg, Heidelberg, Germany

H. WAHL, CERN, Geneva, Switzerland

#### REFERENCES

- 1 N. Kroll, T.D. Lee and B. Fumino, Phys. Rev. 157, 1376 (1967).
- 2 Ye. B. Zel'dovick, Soviet Phys. JETP 36, 984 (1956).
- 3 H. Foeth et al, Physics Letters 30B, 276 (1969).

The neutral kaon is expected to have a short range electromagnetic interaction which can be characterized by a charge radius  $R$ . On the basis of one particular model,<sup>1</sup>  $\langle R^2 \rangle$  is expected to be  $0.76 \times 10^{-27} \text{ cm}^2$ . This interaction gives rise to a  $K^0$ -e scattering amplitude. For kinematic reasons, this amplitude is confined to laboratory angles less than  $\sim \frac{me}{m_k} \approx 10^{-3}$ . The cross section is too small to offer much hope of direct measurement at present. However, the interference between the forward regeneration amplitude so produced, and the nuclear regeneration, should be detectable.<sup>2</sup>

If  $f_{21_e}$  is the electron regeneration amplitude in the forward direction for all the electrons of an atom, and  $f_{21_n}$  is the nuclear regeneration amplitude for the same atom, then the transmission regeneration effect is dominated by  $|f_{21_n} + f_{21_e}|^2$ , whereas the diffraction regeneration is dominated by  $|f_{21_n}|^2$  alone. That is, electron regeneration contributes coherently to transmission regeneration, but not to diffraction regeneration. The method consists in comparing the intensity of transmission regeneration to the differential cross section for diffraction regeneration, extrapolated to zero angle.

$f_{21_e}$  is much smaller than  $f_{21_n}$ , and this is the heart of the experimental problem. In the one previous and

unsuccessful attempt to find this interaction,  $|f_{21_e}/f_{21_n}|$  was found to be  $(1.3 \pm 2.0)\%$ .<sup>3</sup> The expectation of the model of Lee et al<sup>1</sup> would have been 1.2% under these conditions.

The advantage offered by NAL is due to the higher kaon momenta.  $f_{21_e}$  is proportional to the momentum, whereas  $f_{21_n}$  is expected to be proportional to the square root of the momentum, if the momentum dependence observed at lower energies and predicted by Regge Pole models extrapolates to the higher momenta.  $|f_{21_e}/f_{21_n}|$  may therefore be expected to be proportional to the square root of the momentum and the effect to be expected at NAL is considerably larger than at lower energies. With the above premises the model would predict  $|f_{21_e}/f_{21_n}| \approx 5\%$  at 60 GeV/c. With our Charpak chamber detector we expect to be able to be sensitive to an effect as small as  $\sim 1/2\%$ , so that the measurement of the kaon charged radius at NAL would have a high probability of achieving a positive result.

The measurement consists in observing the time dependence and angular dependence of the regeneration produced in a few centimeters of uranium. The beam and apparatus are identical to those of the hydrogen regeneration experiment. A total additional running time of  $\sim 2$  weeks should be sufficient.